AOD and Angstrom exponent of aerosols observed by the Chinese Sun Hazemeter Network from August 2004 to September 2005

Jinyuan Xin[1,3], Yuesi Wang[1,3], Zhanqing Li[2], Pucai Wang[1], Wei-Min Hao[4], Bryce L. Nordgren[4], Shigong Wang[3], Guangren Liu[1], Lili Wang[1], Tianxue Wen[1], Yang Sun[1], Bo Hu[1]

[1] Institute of Atmospheric Physics, Chinese Academy of Sciences, Beijing 100029, P.R.China;

[2] Department of Meteorology, The University of Maryland, College Park, MD 20782, USA;

[3] College of Atmospheric Science, Lanzhou University, Lanzhou 730000, P.R.China;

[4] USDA Forest Service Fire Sciences Laboratory, Missoula, MT 59807, USA

Revised Manuscript Submitted to the Special Issue on

East Asian Study of Tropospheric Aerosols: an International Regional Experiment (EAST-AIRE)

Journal of Geophysical Research – Atmosphere

Submitted: January 26, 2006

Revised: April 6, 2006

Revised: June 6, 2006

Abstract:

To reduce uncertainties in the quantitative assessment of aerosol effects on regional climate and environmental changes, extensive measurements of aerosol optical properties were made with hand-held sunphotometers in the Chinese Sun Hazemeter Network (CSHNET) starting in August 2004. Regional characteristics of the Aerosol optical depth (AOD) at 500 nm and Angstrom exponent (α) computed using 405, 500 and 650 nm were analyzed for the period of August 2004 to September 2005. The smallest mean AOD (~0.15) was found in the Tibetan Plateau where α showed the largest range in value (0.06 - 0.9). The remote northeast corner of China was the next cleanest region with AODs ranging from 0.19 to 0.21 and with the largest α (1.16 - 1.79), indicating the presence of fine aerosol particles. The forested sites exhibited moderate values of AOD (0.19 - 0.51) and α (0.97 - 1.47). A surprising finding was that the AOD measured at a few desert sites in northern China were relatively low, ranging from 0.24 to 0.36, and that α ranged from 0.42 to 0.99, presumably because of several dust-blowing episodes during the observation period. The AOD observed over agricultural areas ranges from 0.38 to 0.90; α ranges from 0.55 to 1.11. These values do not differ much from those observed at the inland urban and suburban sites where AOD ranges from 0.50 to 0.69 and α ranges from 0.90 to 1.48. Given the geographic heterogeneity and the rapid increase in urbanization in China, much longer and more extensive observations are required.

1. Introduction

Atmospheric aerosols play an important role in global and regional climate change [*IPCC*, 1996, 2001; *Haywood and Boucher*, 2000]. In recent years, some findings have shown that aerosols have a significant impact on the solar energy budget and the formation and distribution of precipitation. For example, the reduction of the solar radiation budget at the surface due to the effect of absorbing aerosols is larger than at the top of the atmosphere [*Li*, 1998; *Satheesh and Ramanathan*, 2000; *Li and Trishchenko*, 2001]. Absorption of solar radiation by black carbon aerosols heats the atmosphere [*Jacobson*, 2001]. Suppression of precipitation was observed by dust storms [*Rosenfeld et al.*, 2001; *Ramanathan et al.*, 2001a], air pollution [*Rosenfeld*, 2000; *Rosenfeld and Woodley*, 2001], and fire smoke plumes [*Rosenfeld*, 2000]. Together, they slowdown the hydrological cycles [*Ramanathan et al.*, 2001a].

Although aerosol particles have a potential climatic importance, they are poorly characterized and understood and thus incur large uncertainties in estimating their climatic effects [*Anderson et al*., 2003]. Unlike the uniformly mixed greenhouse gases, tropospheric aerosol properties and effects exhibit considerable spatial and temporal variability [*Streets et al.*, 2001; *Lelieveld et al.*, 2001; *Dickerson et al.*, 2002], of which we have rather poor knowledge and understanding [*IPCC*, 2001; *Satheesh and Moorthy*, 2005]. Aerosol measurements are needed in order to (1) provide validation data for model testing and (2) contribute basic information necessary for improving the assessment of the impact of aerosols on climate forcing [*Chin et al.*, 2002].

Asian aerosol sources differ from those in Europe and North America. In Asia,

there are substantially more coal and biomass burning and dust storms, adding more absorbing soot and organic aerosols to the Asian and Pacific atmospheres [*Streets et al.*, 2001; *Lelieveld et al.*, 2001; *Huebert et al.*, 2003; *Li*, 2004; *Seinfeld et al.*, 2004]. China, the primary source of both natural and anthropogenic aerosols in eastern Asia, is drawing much scientific attention [*Hayasaka et al.*, 2006; *Li*, 2004]. There have been several field projects established to study aerosol characteristics over the south and east Asian regions and their effect on climate, e.g. INDOEX [*Ramanathan et a*l., 2001b], APEX [*Nakajima et al.*, 2003; *Takemura et al.*, 2003], ACE/Asia [*Huebert et al.*, 2003; *Seinfeld et al.*, 2004] and TRACE-P [*Streets et al.*, 2001]. Chinese scientists have also conducted many aerosol-related investigations [*Luo et al.*, 1998; *Mao et al.*, 2002; *Qiu et al.*, 2003], including the use of satellite data to retrieve aerosol optical properties over China [*Li et al.*, 2003a; *Li et al.*, 2003b; *Xiu et al.*, 2003]. Validation of aerosol products obtained from various satellite sensors requires ground-based measurements of a variety of aerosol optical characteristics with different data quality requirements [*Li et al.*, 2003a; *Kaufman and Holben*, 2000; *Dubovik et al.*, 2000]. Due to a lack of systemic and long-term aerosol ground-based measurements, there are still many difficulties and uncertainties when it comes to understanding and explaining the Chinese aerosol issues.

The amassing of continuous aerosol measurements is one of the most powerful ways of monitoring regional aerosol properties, calibrating satellite remote sensing instruments and testing model results [*Huebert et al.*, 2003; *Holben et al.*, 1998]. As a part of the East Asian Study of Tropospheric Aerosols, an International Regional

Experiment (EAST-AIRE) [*Li et al.*, 2006a], the Chinese Sun Hazemeter Network (CSHNET) was initiated in August 2004 by the Institute of Atmospheric Physics, under the auspices of the Chinese Academy of Sciences, the U.S. Forest Service and the University of Maryland. The network is co-located with the Chinese Ecosystem Research Network (CERN), which has sites located in diverse ecosystems in China. Data from this network provide routine observations of aerosol optical properties in the morning and afternoon close to satellite overpass times for validating the satellite products, in addition to charactering the regional aerosol properties.

2. Observation Network and Instrument Calibration

The CSHNET is the first standard network established to measure aerosol optical properties and their spatial and temporal variations throughout China. Figure 1 shows the locations of the sites in the CSHNET. This network includes nineteen CERN stations representing some typical ecosystems, four urban sites, one data collection/processing center and one instrument calibration center. The CERN stations were installed in remote areas in order to represent large-scale regional conditions of certain ecosystems; the urban sites represent typical urban environments. The calibration center is located in Xianghe where annual calibrations of the hazemeters against CIMEL sunphotometers are performed. Data collection and quality control are conducted at the atmosphere sub-center/CERN in Beijing.

The sun hazemeters were manufactured by the U.S. Forestry Service and have been used in some regional aerosol experiments [*Hao et al.*, 2005]. Similar handheld

hazemeters have been widely used for measuring aerosol properties [*Mims*, 1992; *Acharya et al.*, 1995; *Brooks and Mims*, 2001; *Acharya*, 2005]. It has four spectral channels: 405 nm, 500 nm, 650 nm, and 880 nm. The full-width half-maximum (FWHM) at 880 nm is about 30 nm and about 5 nm at the other wavelengths. The field of view is about 2.5º. Measurements are taken more than 20 times a day, and the observation period is from 10AM to 2PM (local time), encompassing MODIS satellite overpass times. The hazemeters use light-emitting diode (LED) detectors in place of optical interference filters and photo diodes. The advantages of using LEDs include low cost, durability, and long-term optical stability [*Brooks and Mims*, 2001; *Acharya*, 2005].

Measurements taken from August 2004 to September 2005 were available from almost all sites. For the retrieval of aerosol optical properties, cloud-contaminated measurements were removed using cloud observation records compiled by observers on the ground. Some uncertainties are introduced in this step because sub-visible cloud can be missed by the human observer. Columnar AODs were estimated using the Beer-Lambert-Bouguer law. To determine the Angstrom exponent, a basic measure related to the aerosol size distribution, a log-linear fitting was applied using three wavelengths (405 nm, 500 nm and 650 nm) [*Kim et al.*, 2004]. In general, the Angstrom exponent ranges from 0.0 to 2.0, with smaller Angstrom exponents corresponding to larger aerosol particle sizes [*Dubovik et al.*, 2002; *Kim et al.*, 2004].

Given their relatively wide and unstable spectral response, periodic calibration of the LED hazemeters is necessary. The LED hazemeters were calibrated using two

standard approaches: the Langley plot calibration and the transfer calibration [*Brooks and Mims*, 2001]. Figure 2 shows Langley plot calibrations for the LED hazemeters at the Lhasa, Fukang, Sanjiang and Beijing sites. Application of the Langley method requires a stable atmosphere during a period of at least several hours. It is impractical to perform time-consuming Langley plot calibrations on large numbers of hazemeters. Transfer calibration is an alternative method using several Langley calibrated hazemeters as reference [*Brooks and Mims*, 2001].

Figure 3 shows a comparison of hazemeter and CIMEL sunphotometer AODs at four wavelengths. Measurements shown were taken at the Beijing (bottom panels) and Xianghe (top panels) sites. The ID041 hazemeter at the Beijing site is calibrated by the Langley method with data from August to December 2004, while the ID005 hazemeter at the Xianghe site is calibrated by the transfer calibration method with data from February to August 2005. The slope of the regression line between the two sets of AOD is close to 1.0 at 405 nm, 500 nm and 650 nm. The hazemeter results are generally consistent with the CIMEL results with disagreements on the order of 2% to 6%. At 880 nm, the hazemeter results show larger errors (on the order of about 12% to 15%) because of the large FWHM at that wavelength, water vapor contamination and observation errors. Although the equipment can reach a certain precision, there is the uncertainty in the estimate with a single measurement. It would be nice to add comparisons with other instruments such as MODIS in future. You should give the standard devistion of the comparison as an indication of errors in individual comparison. Note that MODIS has much large errors than ground-based sun

photometer measurements. So, the last statement is not right.

3. Results and Discussion

The annual mean values of AOD and α are delineated in Table 1. Figure 4 shows the time series of daily mean AOD at 500 nm and the scatterplots of α against AOD at two sites on the Qinghai-Tibet Plateau from August 2004 to September 2005. As expected, both sites have very clean air with low and stable AOD. The annual means and standard deviations of the AOD are 0.14±0.08 and 0.15±0.07 at the Lhasa and Haibei stations, respectively; the annual mean α is 0.06±0.31 and 0.90±0.52, respectively. At Haibei, α varies greatly over a narrow range of AOD, implying different types of aerosols. There is an increase in small aerosol particles during autumn and winter due to regional biomass burning. In the spring and summer seasons, large continental/dust aerosol particles dominate. This suggests that more than one type of aerosol is required in climate models to adequately represent their climatic effects. The unusually low values of α are questionable and are subject to large uncertainties due to the very low AOD [*Jeong et al.*, 2005].

Figure 5 is the same as Figure 4 but for the far northeast corner of China, the second cleanest region among all the regions studied here. The annual mean AOD at 3 sites (Hailun, Sanjiang and Changbai Mountain) is around 0.2±0.10 and α at all sites decreases with increasing AOD. Both AOD and α exhibit large and distinct seasonal trends, implying a systematic seasonal shift in aerosol type. The aerosol particle size decreases from autumn to winter, presumably due to increases in biomass and fossil

fuel burning as the winter season approaches. Meanwhile, a gradual increase in snow and ice cover on the ground prevents soil erosion and thus restricts the emission of coarse-mode mineral particles, which is also implied by the low AOD during this season. An opposite trend is observed from winter to spring where increasing AOD and decreasing α is evident. In spring and summer, the aerosols seem to be more of a continental variety.

Figure 6 presents the same results at two forest stations, one in northern China (Beijing Forest station) and another in southern China (Xishuangbanna station). There are large differences between the two stations both in terms of the magnitudes and seasonal variations of AOD and α, as well as the dependence of α on AOD. The general trends of AOD and α at the Beijing Forest station bear a close resemblance to those observed at the three northeast sites except that the AOD is generally larger with many short-term episodes of very high AOD. This site is influenced by regional aerosol emission sources from Beijing and Hebei, Inner Mongolia and Shanxi provinces. In winter, the site is overwhelmed by smoke aerosols from biomass burning. Drastic changes in AOD were usually caused by changes in airmass due to the passage of cold fronts, which were also observed at the supersite in Xianghe by various instruments measuring aerosol, gases, cloud and radiation quantities [*Li et al.*, 2006a, b, submitted to the same EAST-AIRE special issue]. The increase in AOD was usually caused by the buildup of anthropogenic pollutants, as indicated by the consistent episodes seen in simultaneous measurements of precursor gases such as SO_2 and CO and NOy made during an intensive observation period conducted during

March 2005 [*Li et al.*, 2006b].

The Xishuangbanna station is located in the tropical forests of Yunnan province in southwest China. The organic aerosols produced by tropical forests impair visibility and increase AOD. During the dry season from November to April, the mean values of AOD and α were 0.59±0.25 and 1.60±0.40, respectively. During the rainy season from May to October, the mean values of AOD and α were reduced to 0.38±0.17 and 1.29±0.38, respectively, which may have been caused by differences in the production and elimination of organic aerosols between dry and rainy seasons.

Figure 7 shows the results at three northern stations representing different desert-like ecosystems. The AODs at these stations are moderately high with annual mean values ranging from 0.24 to 0.36; α varies from 0.42 to 0.99. The Shapotou site, situated in an arid part of the Tengger Desert. Dust storm frequency and precipitation amounts were below average during the period [*Xin et al., 2005*] possibly resulting in smaller seasonal changes in AOD than normal. The Fukang station is located in the transition zone from a glacial environment to a desert environment and the Eerdousi station is situated in a sandy grassland ecosystem within a semi-arid region. The Fukang and Eerduosi sites have more vegetation on the ground so there is less aerosol emission than at the Shapotou site. Also, agricultural and pastoral activities take place in the regions surrounding the Fukang and Eerduosi sites, leading to changes in dominant aerosol types during the year. Aerosol particles are small during autumn and winter because of biomass burning by the local farmers. Given that the sole source of aerosols in the more desert-like region is natural dust emission, dust aerosols are more

persistent at the Shapotou station.

The results obtained at three stations near large water bodies (Lake Tai, Jiaozhou Bay, and Shanghai City) are presented in Figure 8. These sites are located along the eastern seashore of China, except for Lake Tai, which is about 130 km to the west of Shanghai. These sites have similar annual mean AOD, ranging from 0.48 to 0.67, as well as similar annual mean α (0.86 - 1.11). However, the Jiaozhou Bay station shows much larger variations in both AOD (0.2 - 1.4) and α (0.2 - 1.8) and the two variables are anti-correlated. This implies that the heavy aerosol loading at this site corresponds to coarse-mode particles, which may result from the humidity-swelling of sea salt aerosols. Due to the close proximity of the Lake Tai and Shanghai stations, the day-to-day variations in AOD and α are similar. In Shanghai, α has little dependence on AOD, which might be an indication of mixed aerosol types. At the Lake Tai station, there is a positive dependence, which may signify the dominant influence of fine-mode pollutants. Note that the region surrounding Lake Tai (more widely known as the Yangzi Delta) is China's leading manufacturing base with thousands of small privately owned factories emitting huge amounts of pollutants. Pinpointing the exact nature of aerosols observed in this or other sites would require many in-situ observations such as those taken during the intensive field campaign conducted in Xianghe [*Li et al.*, 2006b].

The results obtained at five agricultural stations are shown in Figure 9. These stations are mostly located throughout a large area of central China dominated by farmland. The annual mean AOD ranges from moderately high to high values:

0.38±0.14, 0.59±0.24, 0.90±0.38 and 0.70±0.26, respectively, for the Ansai, Fengqiu, Yanting and Taoyuan stations. The annual mean α is approximately equal to 1 with a standard deviation of ~0.28 for all the stations, except for Ansai where α is 0.55±0.46. More mineral dust aerosols are emitted in this region, due to intensive farming and the exposure of bare soil. The day-to-day variation of AOD is large, but its seasonable dependence is weak. The intermittently high AODs originate most likely from blowing dust. Yanting, located in the basin of Sichuan Province, has the largest AOD; Ansai, located in the Loess Plateau of Shanxi Province, has the lowest AOD.

Results obtained at a few major Chinese cities are presented in Figure 10. Measurements taken at the Shenyang station, an agricultural site located in a suburb of Shenyang City; show that the air is mostly urban in character. Comparisons with results for the rural agricultural sites (Figure 9) highlight some interesting features. Overall, the annual mean AOD are similar for both urban and rural sites, which is contrary to common belief. Also, the day-to-day variations of AOD for the urban sites are substantially larger than the rural sites, both in terms of the magnitude and frequency of changes. At the Lanzhou City site in midland China, α does not change much with the AOD due to the strong influence of dust aerosol and pollutants generated from ground surface emissions and transportation of dust from other arid desert regions in northwest China. The AOD is large (0.79) and α is small (0.84) in winter and spring, compared to summer and autumn. The seasonal variation stems from both emission strength and atmospheric dynamic conditions. Lanzhou is a major industrial city in northwest China, situated in a local basin with frequent temperature

inversions during the winter. Heavy aerosols generated by windswept dust, winter heating, and industrial activities are often trapped in the basin during winter when rainfall amounts are minimal, making it one of the most polluted regions in China.

There are two stations in Beijing, one near the city center and another in a distant suburb (Xianghe) about 70 km east of Beijing City. The suburban site has slightly lower AODs than the city site. At both stations, the AOD values are large and fluctuate much more than those observed in Lanzhou. Another distinct feature in Beijing is that there were some very clean days with AODs less than 0.2 and very turbid days with AODs ranging from 1.5-4 [*Li et al.*, 2006a] that occurred alternatively over short periods of time. Explanations for this phenomenon were given earlier. Moreover, α also exhibits a large variation but is generally larger than Lanzhou, presumably due to a much lower concentration of dust aerosols in Beijing. In general, aerosols in Beijing are much more diverse than in Lanzhou, encompassing the very fine-mode aerosols from fossil fuel burning and biomass burning to large coarse-mode dust aerosols originating from the desertification grassland in Mongolia. During the first month of the lunar year, smoke aerosols were detected, emanating from the firework displays celebrating the Chinese New Year. From spring to summer, the AOD increases because of at least in part humidity swelling [*Li et al.*, 2006a; *Jeong et al.*, 2006].

Some intriguing findings can be seen by comparing the aerosol characteristics measured at the Lanzhou and Shenyang sites, located in major industrial zones in northeast and northwest China. Both stations show large AODs, but their seasonal

trends appear to be opposite. In Shenyang, the AOD is generally high in summer and low in winter, whereas in Lanzhou, the trend is opposite. This is because Shenyang is close to the Yellow Sea and the humidity in summer is high, leading to a stronger humidity effect and larger AOD. In wintertime, cold air from Siberia often brought clean air into the region, washing away pollutants. These arguments are supported by the seasonal change in α: smaller (large particles) in summertime and larger (smaller particles) in wintertime, also opposite to the seasonal change in Lanzhou.

4. Conclusions

As a summary of the study, Figure 11 shows the nation-wide distribution of aerosol optical depth (AOD) at 500 nm and the Angstrom exponent (α) during the four seasons as measured by the Chinese Sun Hazemeter Network (CSHNET). The CSHNET is the first large-scale network measuring AOD directly at multiple wavelengths on a routine basis for long-term monitoring and characterization of aerosols in China. Overall, AODs are larger in central and southeast China. There are many anthropogenic sources of aerosols in southeast China. Sites located in the Qinghai-Tibet Plateau and the far northeast corner of China are the cleanest among all sites under study. In late autumn and winter, the majority of observation sites in northern China are under the influence of coal burning and biomass and fossil fuel burning which produce heavy loadings of fine-mode aerosols. From spring to summer, many eastern stations experience rises in AOD and decreases in α due to the humidity-swelling effect. Desert or desert-like stations in western China are more

affected by the coarse-mode mineral dust aerosols, with the peaks of loading in spring. Continental aerosols are observed across China because of dust transportation and relatively strong regional emissions, while pollutants may play a more significant role in urban regions. Many sites in eastern China show aerosol properties characteristic of mixtures of pollutants, mineral aerosols, and smoke aerosols. One finding worth noting is that the aerosol loading is generally heavy in many parts of China but seems not to differ significantly between rural agricultural stations and urban stations, at least for the stations under study. The annual mean AOD averaged over all the sites is 0.43, which is about 3 times the global mean value measured at all the Aerosol Robotic Network sites [*Dubovik et al.*, 2002] .

Acknowledgments. This work was partly supported by the Project of Field Station Network of the Chinese Academy of Sciences, the National Natural Science Foundation of China (40525016; 40520120071), and the NASA Radiation Science Program (NNG04GE79G). The authors thank the Chinese Ecosystem Research Network (CERN) and the U.S. Forestry Service for contributions to this research. The paper was edited by Maureen Cribb.

References

Acharya, Y. B. (2005), Spectral and emission characteristics of LED and its application to LED-based sun-photometry, *Optics & Laser Technology*, *37*, 547-550.

Acharya, Y. B., A. Jayaraman, S. Ramachandran, B. H. Subbaraya (1995), Compact light emitting diode sun photometer for atmospheric optical depth measurement, *Appl. Opt.*, *34*(7), 1209-1214.

Anderson, T., R. J. Charlson, S. E. Schwartz, R. Knutti, O. Boucher, H. Rodhe, and J. Heintzenberg (2003), Climate forcing by aerosols: A hazy picture, *Science*, *300*, 1103-1104.

Brooks, D. R., and F. M. III Mims (2001), Development of an inexpensive handheld LED-based Sun photometer for the GLOBE program, *Journal Geophys. Res.*, *106*(D5), 4733-4740.

Chin, M., Ginoux, P., Kinne, S., Torres, O., Holben, B., Duncan, B. N., Martin, R. V., Logan, J. A., Higurashi, A., and Nakajima, T.: Tropospheric aerosol optical thickness from the GOCART model and comparisons with satellite and sun photometer measurements, *J. Atmos., Sci*., 59, 461-483, 2002.

Dickerson, R. R., M. O. Andreae, T. Campos, O. L. Mayol-Bracero, C. Neususess, and D. G. Streets (2002), Analysis of black carbon and carbon monoxide observed over the Indian Ocean: Implications for emissions and photochemistry, *J. Geophys. Res.*, *107* (D19), 8017.

Dubovik, O., A. Smirnov, B. N. Holben, M.D. King, Y. J. Kaufman, T. F. Eck, and I. Slutsker (2000), Accuracy assessments of aerosol optical properties retrieved from Aerosol Robotic Network (AERONET) sun and sky radiance measurements. *J. Geoph. Res.*, *105*(8), 9791-9806.

Dubovik, O., B. N. Holben, T. F. Eck, A. Smirnov, Y. J. Kaufman, M. D. King, D. Tanre, and I. Slutsker (2002), Variability of absorption and optical properties of key aerosol types observed in worldwide locations, *J. Atmos. Sci.*, *59*, 590-608.

Hao, W.M., D.E. Ward, R.A. Susott, R.E. Babbitt, B.L. Nordgren, Y.J. Kaufman, B.N. Holben, and D.M. Giles (2005), Comparison of aerosol optical thickness measurements by MODIS, AERONET sun photometers, and Forest Service handheld sun photometers in southern Africa during the SAFARI 2000 campaign, *Int. J. Remote Sensing*, *26*, 4169-4183.

Hayasak, T., K. Kawamoto, G. Shi, A. Ohmura (2006), Importance of aerosols in satellite-derived estimates of surface shortwave irradiance over China, Geophy. Res. Lett., 33, 10.1029/2005GL025093.

Haywood, J.M., and O. Boucher (2000), Estimates of the direct and indirect radiative forcing due to tropospheric aerosols: a review, *Revs. Geophys.*, *38*, 513-543.

Holben, B. N., et al. (1998), AERONET - A federated instrument network and data archive for aerosol characterization, *Remote Sensing of Environment*, *66*(1), 1-16.

Huebert, B. J., T. Bates, P. B. Russell, G. Shi, Y. J. Kim, K. Kawamura, G. Carmichael, T. Nakajima (2003), An overview of ACE-Asia: Strategies for quantifying the relationships between Asian aerosols and their climatic impacts, *J. Geophys. Res.*, *108* (D23), 8633.

Intergovernmental Panel on Climate Change (IPCC) (2001), Climate Change 2000, The Scientific Basis-Contribution of Working Group I to the Third Assessment Report of the Intergovernmental Panel on Climate Change. Cambridge University Press, New York.

Intergovernmental Panel on Climate Change (IPCC) (1996), Climate Change 1995, The science of climate change, contribution of working group I to the second assessment report of the IPCC. Cambridge University Press, Cambridge, UK.

Jacobson, M.Z. (2001), Strong radiative heating due to the mixing state of black carbon in atmospheric aerosols, *Nature*, *409*, 695-697.

Jeong, M.J , Z. Li, D.A. Chu, and S-T. Tsay (2005), Quality and Compatibility Analyses of Global Aerosol Products Derived from the Advanced Very High Resolution Radiometers and the Moderate Imaging Spectroradiometer, *J. Geophy. Res.*, 110, D10S09, doi:10.1029/2004JD004648.

Jeong, M.-J., Z. Li, S.C. Tsay, (2006), Effect of Aerosol Humidification on the Column Aerosol Optical Thickness over the ARM Southern Great Plains Site, J. Geophy. Res., submitted.

Kaufman, Y. J., B. N. Holben (2000), Will aerosol measurements from Terra and Aqua polar orbiting satellites represent the daily aerosol abundance and properties? *Geophysics Research Letters*, *27* (23), 3861-3864.

Kim, D., B. Sohn, T. Nakajima, T. Takamura, T. Takemura, B. Choi, and S. Yoon (2004), Aerosol optical properties over East Asia determined from ground-based sky radiation measurements, *J. Geophys. Res.*, *109*, D02209.

Lelieveld, J., et al. (2001), The Indian Ocean Experiment: Widespread air Pullution from South and South-East Asia, *Science*, *291*(5506), 1031-1036.

Li, C., et al. (2003a), Characteristics of distribution and seasonal variation of aerosol optical depth in eastern China with MODIS products, *Chinese Science Bulletin*, *48*(22), 2488-2495.

Li, X., Y. Liu, H. Qiu, Y. Zhang (2003b), Retrieval method for optical thickness of aerosols over Beijing and its vicinity by using the MODIS data, *ACTA METEOROLOGICA SINICA*, *61*(5), 581-592. (In Chinese)

Li, Z. (1998), Influence of absorbing aerosols on the inference of solar surface radiation budget and cloud absorption, *J. Climate, 11*, 5-17.

Li, Z. (2004), Aerosol and climate: A perspective from East Asia, In "Observation, Theory, and Modeling of the Atmospheric Variability" (ed. Zhu), *World Scientific Pub. Co.*, 501-525.

Li, Z., A. Trishchenko (2001), Quantifying the uncertainties in determining SW cloud radiative forcing and cloud absorption due to variability in atmospheric condition, *J. Atmos. Sci.*, *58*, 376-389.

Li, Z., et al. (2006a), Aerosol optical properties and radiative effects in Northern China. submitted to the same EAST-AIRE special issue.

Li, C., et al. (2006b), In-Situ Measurements of Trace Gases and Aerosol Optical Properties at a Rural Site in Northern China during EAST-AIRE IOP 2005. submitted to the same EAST-AIRE special issue.

Luo, Y., X. Zhou, W. Li (1998), Advances in the study of atmospheric aerosol radiative forcing and climate change, *Advance in earth sciences*, *13*(6), 572-581. (In Chinese)

Mao, J., J. Zhang, M. Wang (2002), Summary comment on research of atmospheric aerosol in china, *ACTA METEOROLOGICA SINICA*, *60*(5), 625-634. (In Chinese)

Mims, F. M. III (1992), Sun photometer with light-emitting diodes as spectrally selective detectors, *Applied Optics*, *31*(33), 6965-6967.

Nakajima, T., et al. (2003), Significance of direct and indirect radiative forcings of aerosols in the East China Sea region. *Journal of Geophysical Research*, *108*(D23), 8658, doi:10.1029/2002JD003261.

Qiu, J., D. Lu, H. Chen, G. Wang and G. Shi (2003), Modern research progresses in atmospheric physics, *Chinese Journal of Atmospheric Sciences*, *27*(4), 628-652. (In Chinese)

Ramanathan, V., P.J. Crutzen, J.T. Kiehl, and D. Rosenfeld (2001a), Aerosols, climate and the hydrological cycle, *Nature*, *294*, 2119-2124.

Ramanathan, V., et al. (2001b), Indian Ocean experiment: An integrated analysis of the climate forcing and effects of the great Indo-Asian haze, *J. Geophys. Res.*, *106*(D22), 28371-28398, 10.1029/2001JD900133.

Rosenfeld, D. (2000), Suppression of rain and snow by urban and industrial air pollution, *Science*, *287*, 1793-1796.

Rosenfeld, D., and W. Woodley (2001), Pollution and clouds, *Physics World*, 33-37.

Rosenfeld, D., Y. Rudich, and R. Lahav (2001), Desert dust suppressing precipitation: A possible desertification feedback loop, *Proceedings of the National Academy of Sciences (PNAS)*, *98*, 5975-5980.

Satheesh, S. K. and K. K. Moorthy (2005), Radiative effects of natural aerosols: A review. *Atmospheric Environment*, *39*(11) 2089-2110.

Satheesh, S.K., and V. Ramanathan (2000), Large differences in tropical aerosol forcing at the top of the atmosphere and Earth's surface, *Nature*, *405*, 60-63.

Seinfeld, J. H., et al. (2004), ACE-ASIA: Regional Climatic and Atmospheric Chemical Effects of Asian Dust and Pollution, *Bulletin of the American Meteorological Society*, *85*(3), 367–380.

Streets, D. G., S. Gupta, S. T. Waldhoff, M. Q. Wang, T. C. Bond, and Y. Bo (2001), Black carbon emissions in China, *Atmos. Environ.*, *35*, 4281-4296.

Takemura, T., T. Nakajima, A. Higurashi, S. Ohta, and N. Sugimoto (2003), Aerosol distributions and radiative forcing over the Asian-Pacific region simulated by Spectral Radiation-Transport Model for Aerosol Species (SPRINTARS). *Journal of Geophysical Research*, *108*(D23), 8659, doi:10.1029/2002JD003210.

Xin, J., S. Wang, Y. Wang, J. Yuan, W. Zhang, Y. Sun (2005). Optical properties and size distribution of dust aerosols over the Tengger Desert in Northern China. *Atmospheric Environment, 39*, 5971-5978.

Xiu, X., et al. (2003), Explore aerosol variational field by using MODIS data and ground-based photometer observation, *Chinese Science Bulletin*, *48*(15), 1680-1685. (In Chinese)

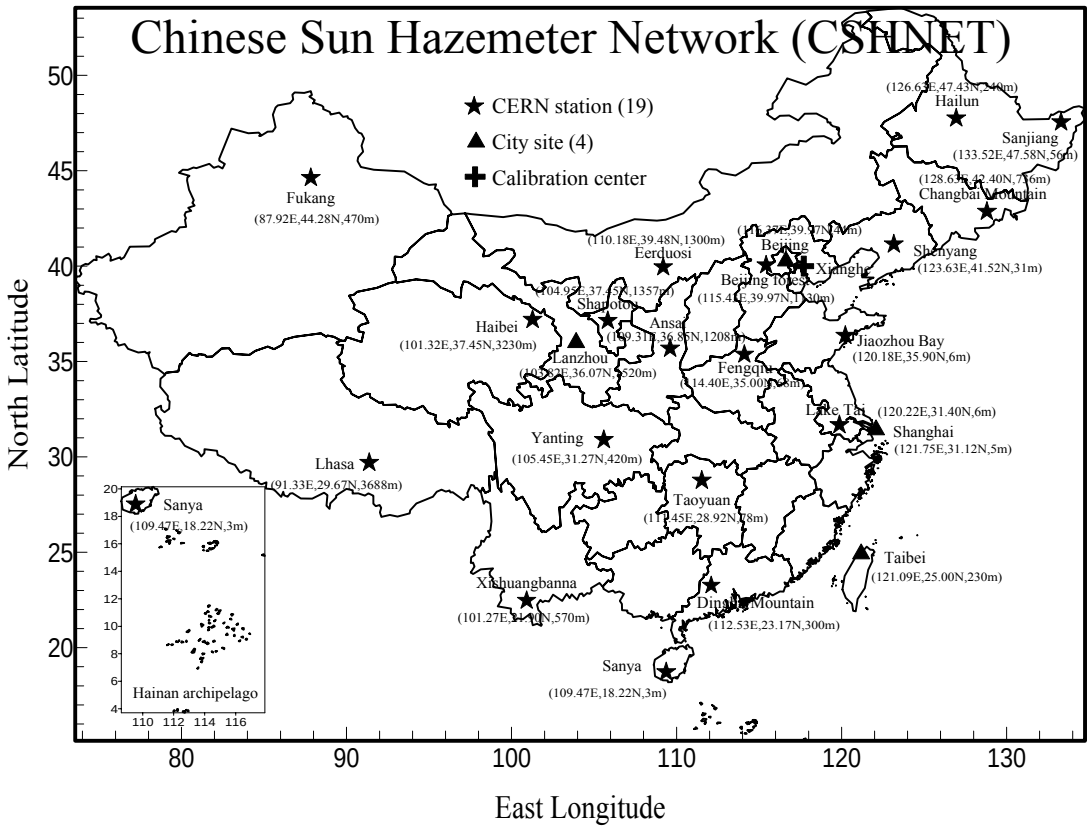

Figure 1. Geographical locations of the CSHNET sites.

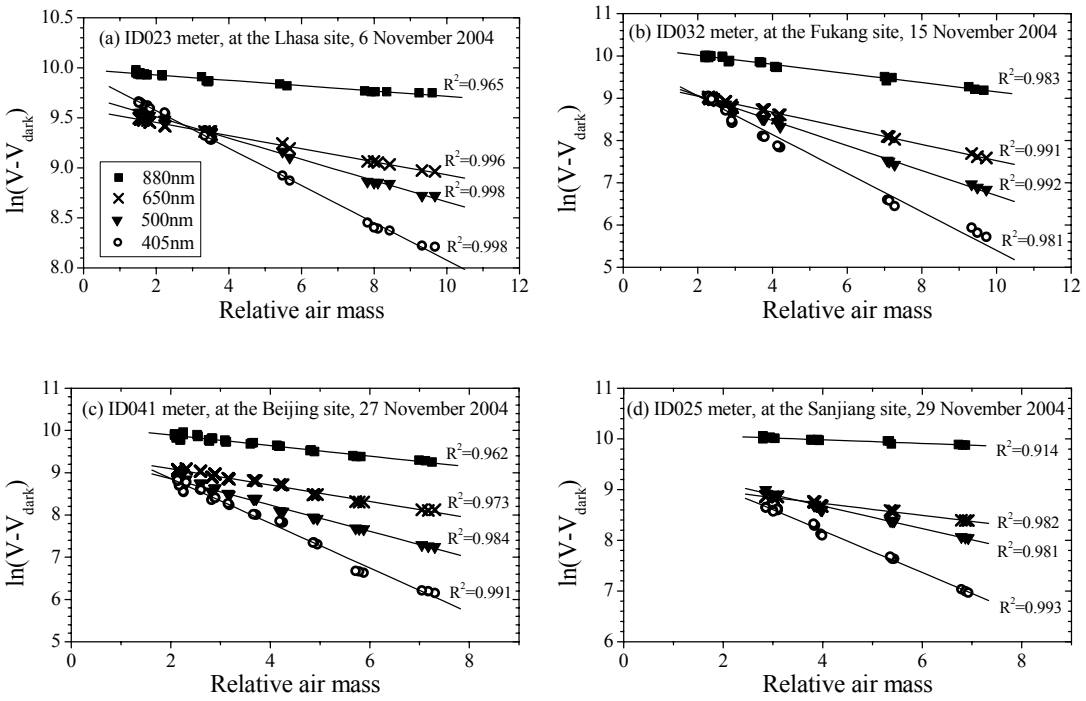

Figure 2. The Langley calibration plots of LED hazemeters at four sites. V and V_{dark} are the sunlight and dark voltages at four specific channels.

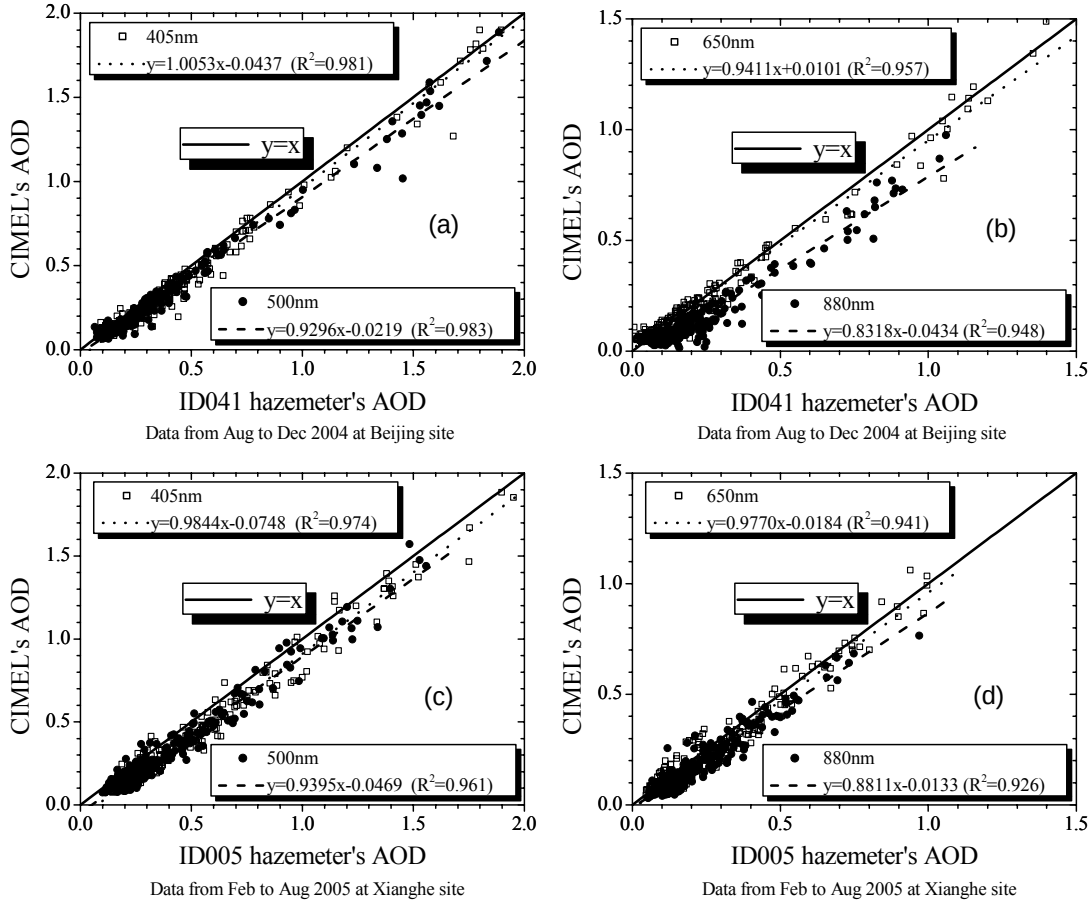

Figure 3. Comparison of AODs measured by CIMEL sunphotometers and hazemeters at two sites.

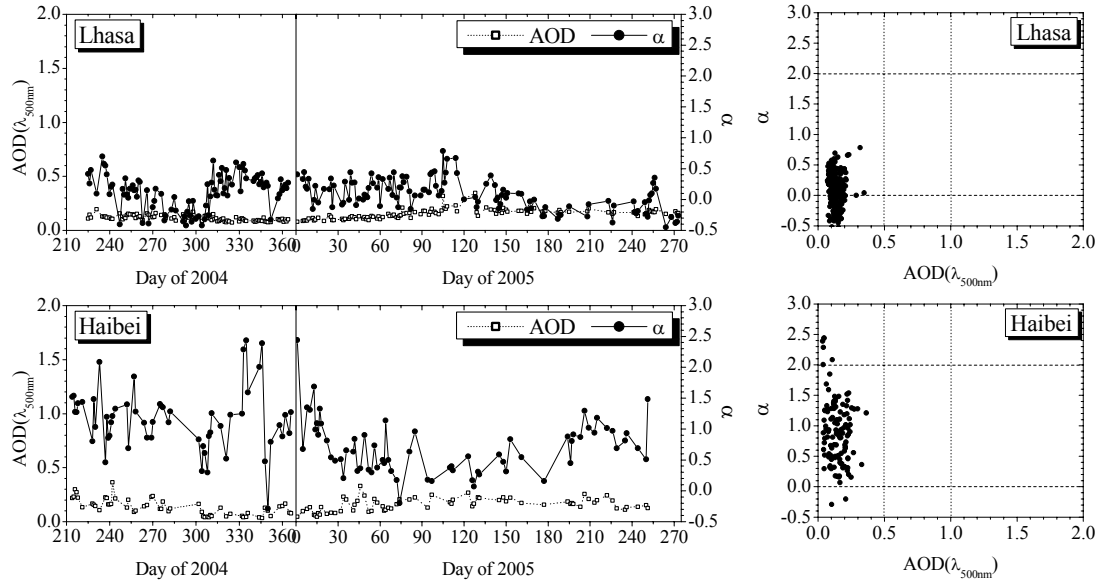

Figure 4. Time series and scatterplots of daily averaged AOD at 500 nm and α at sites on the Qinghai-Tibet Plateau.

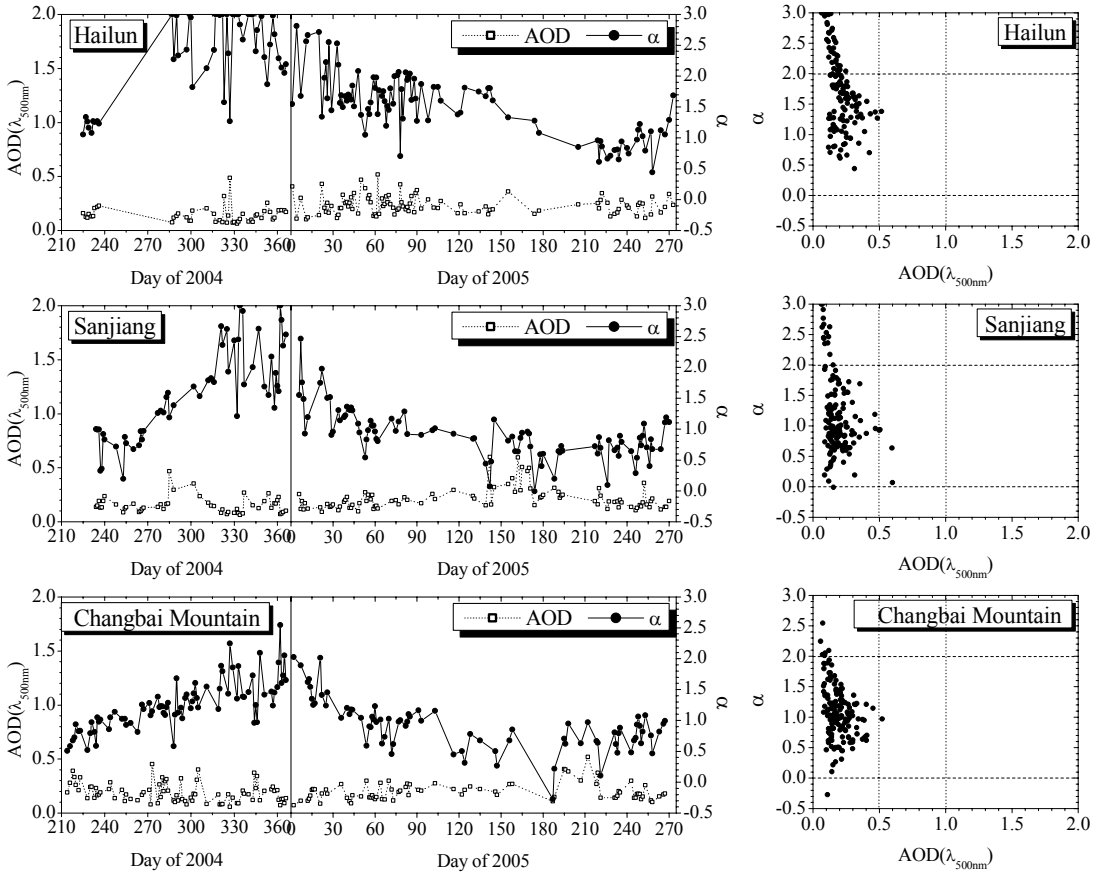

Figure 5. Time series and scatterplots of daily averaged AOD at 500 nm and α at sites in northeast China.

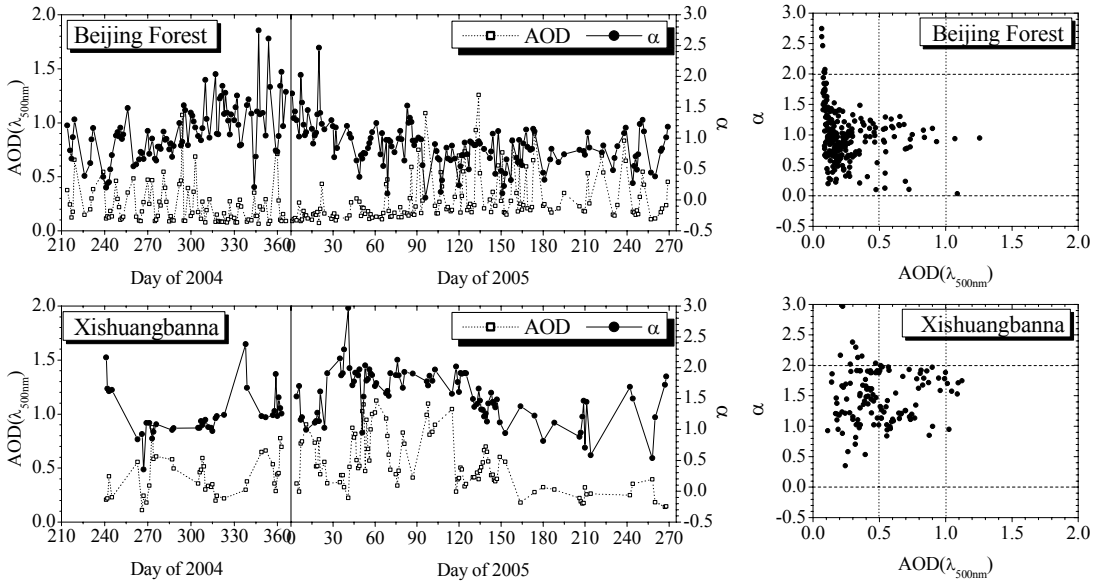

Figure 6. Time series and scatterplots of daily averaged AOD at 500 nm and α at forest stations.

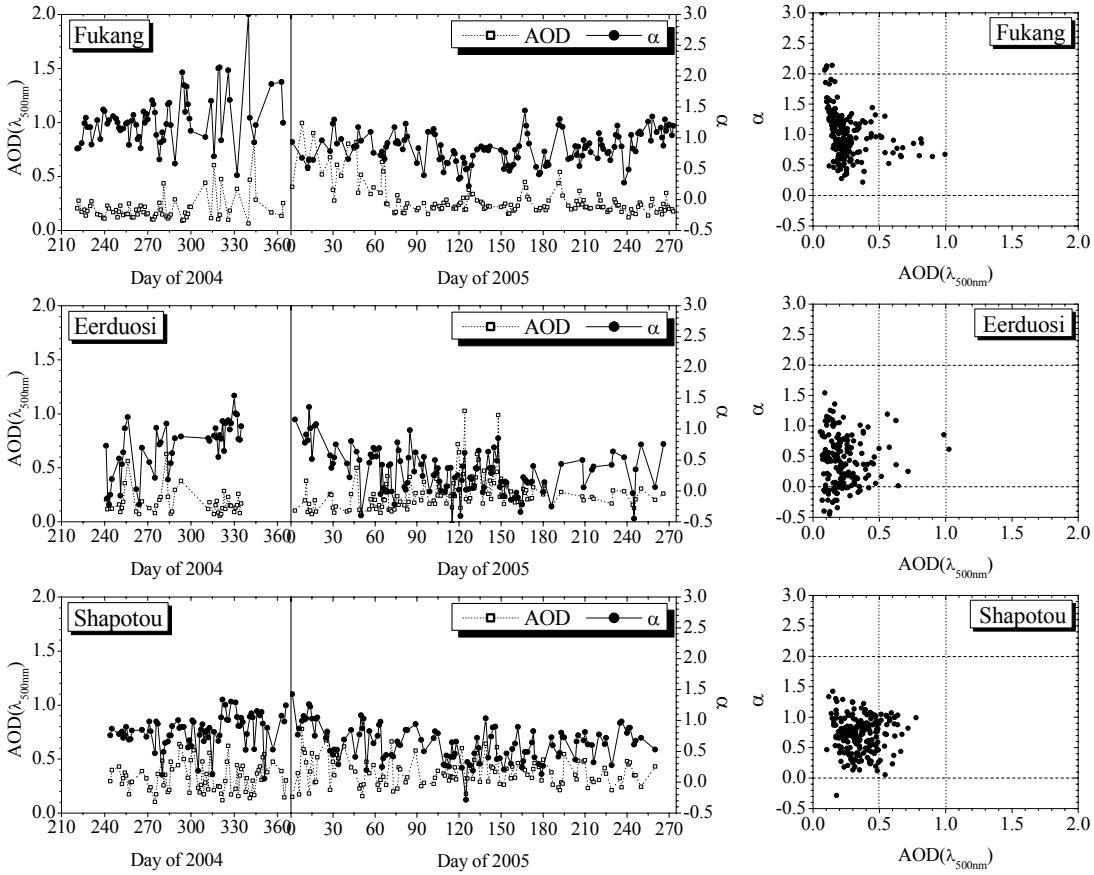

Figure 7. Time series and scatterplots of daily averaged AOD at 500 nm and α at northern desert stations.

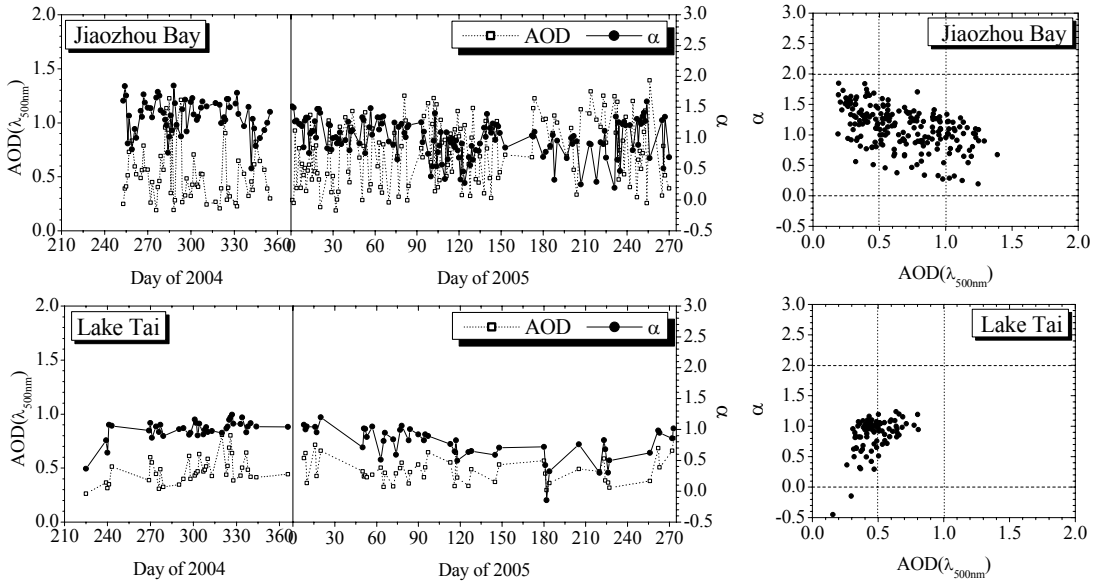

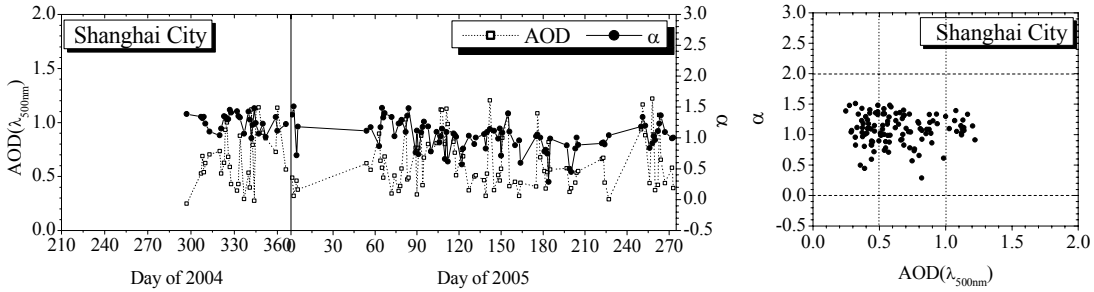

Figure 8. Time series and scatterplots of daily averaged AOD at 500 nm and α at stations along the East Sea.

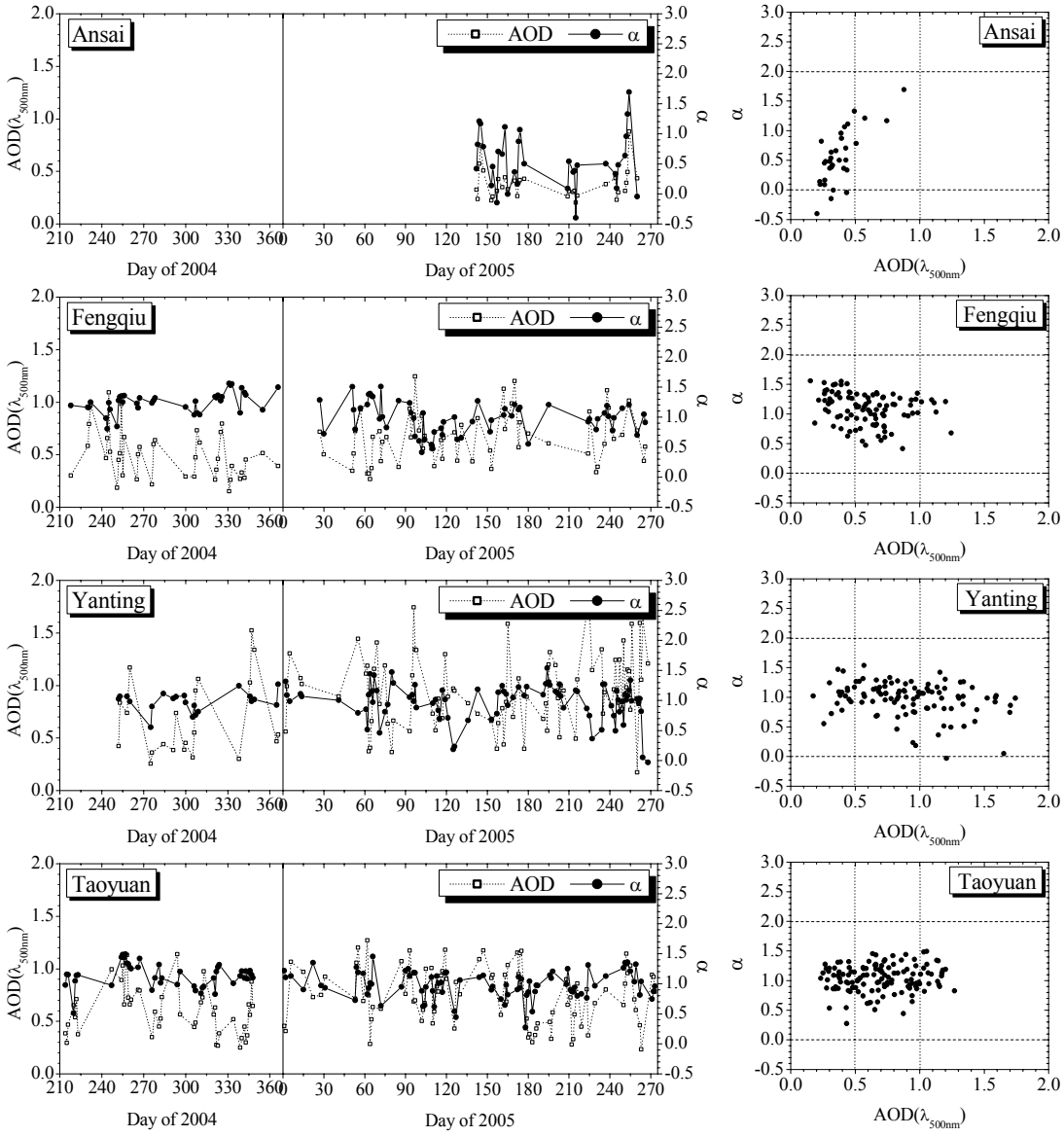

Figure 9. Time series and scatterplots of daily averaged AOD at 500 nm and α at agricultural stations.

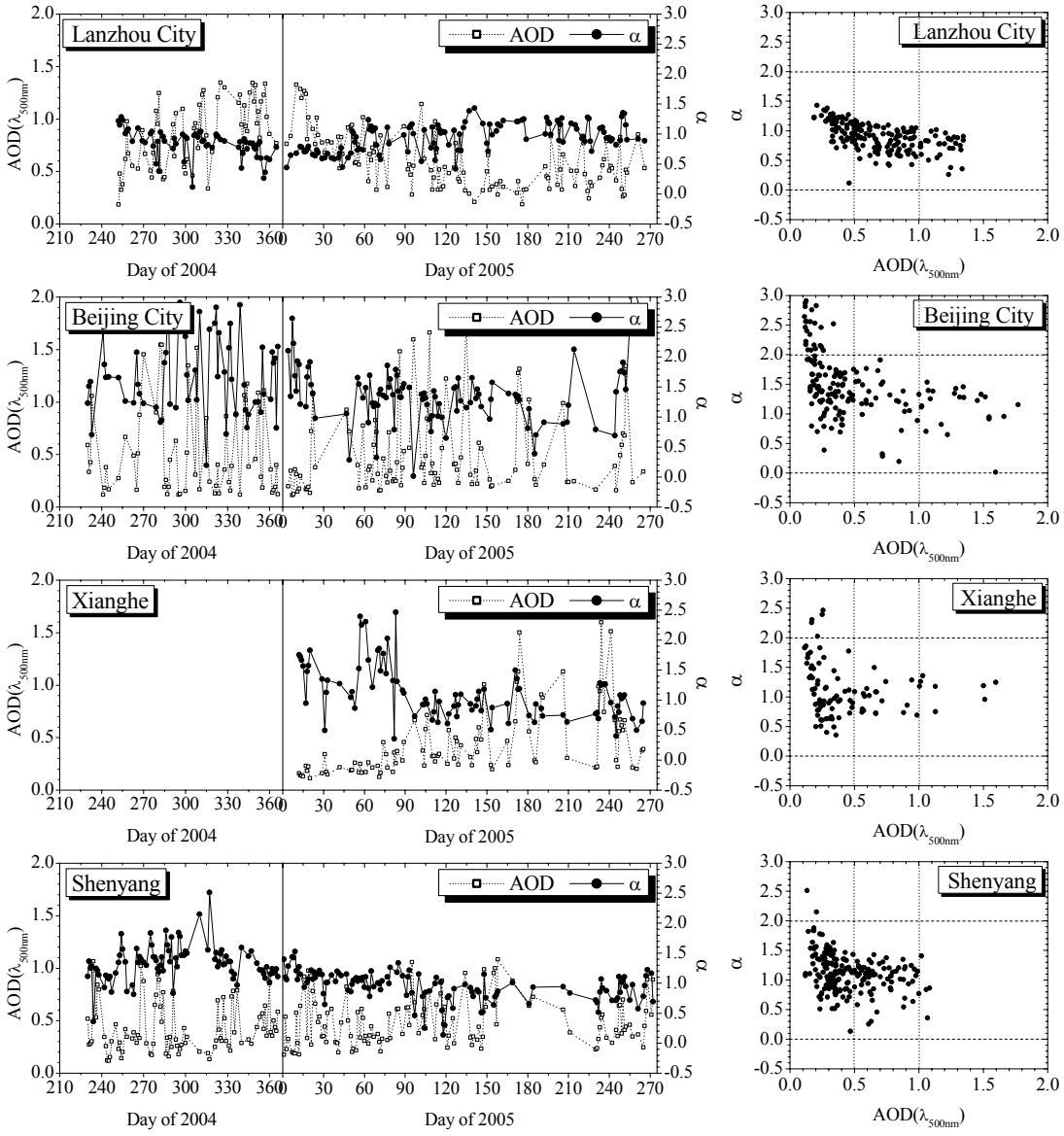

Figure 10. Time series and scatterplots of daily averaged AOD at 500 nm and α at urban and suburban stations.

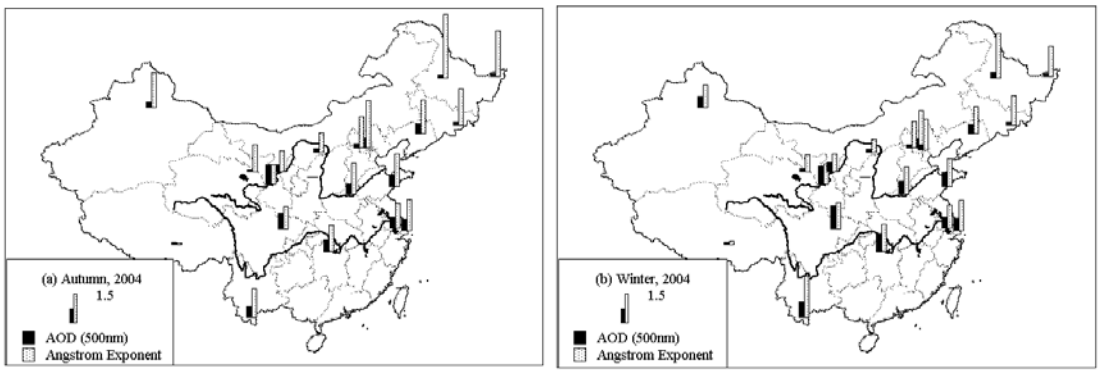

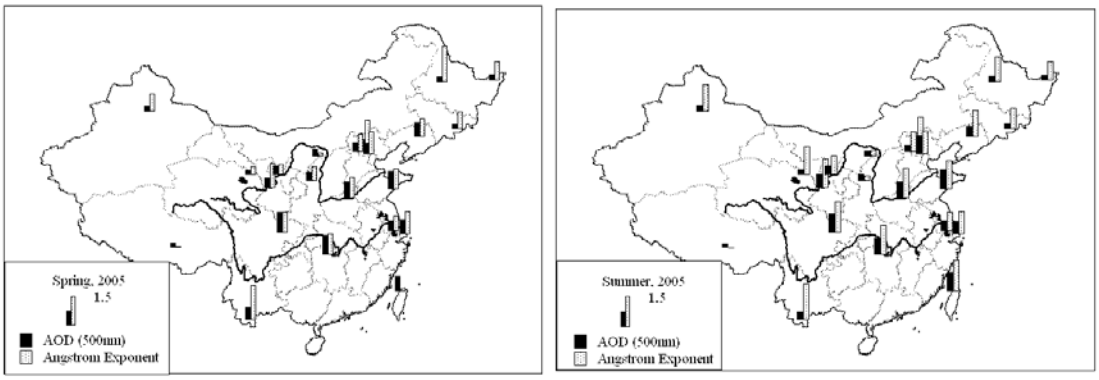

Figure 11. Plots of seasonally-averaged AOD at 500 nm and α measured at sites in the CSHNET.

Table 1. The annual means and standard deviations of AOD at 500 nm and α measured at sites in the CSHNET.

The site name	Ecosystem	Longitude	Latitude	AOD	α
Lhasa	Plateau agriculture	91.33	29.67	0.14±0.08	0.06±0.31
Haibei	Plateau grassland	101.32	37.45	0.15±0.07	0.90±0.52
Hailun	Marsh	126.63	47.43	0.21±0.09	1.79±0.68
Sanjiang	Agriculture	133.52	47.58	0.19±0.10	1.16±0.63
Changbai Mountain	Forest	128.63	42.40	0.19±0.08	1.09±0.44
Beijing Forest	Forest	115.43	39.96	0.26±0.20	0.97±0.42
Xishuangbanna	Forest	101.27	21.90	0.51±0.24	1.47±0.42
Fukang	Desert	87.92	44.28	0.26±0.15	0.99±0.38
Eerduosi	Desert	110.18	39.48	0.24±0.15	0.42±0.41
Shapotou	Desert	104.95	37.45	0.36±0.13	0.71±0.29
Jiaozhou Bay	Marginal sea	120.18	35.90	0.67±0.30	1.11±0.33
Lake Tai	Lake	120.22	31.40	0.48±0.12	0.86±0.28
Shanghai	Urban	121.75	31.12	0.64±0.25	1.08±0.24
Ansai	Agriculture	109.31	36.85	0.38±0.14	0.55±0.46
Fengqiu	Agriculture	114.40	35.00	0.59±0.24	1.09±0.26
Yanting	Agriculture	105.45	31.27	0.90±0.37	0.98±0.28
Taoyuan	Agriculture	111.45	28.92	0.70±0.26	1.04±0.23
Lanzhou	Urban	103.82	36.07	0.69±0.30	0.90±0.23
Beijing	Urban	116.37	39.97	0.50±0.39	1.48±0.56
Xianghe	Suburban	116.96	39.75	0.44±0.32	1.12±0.44
Shenyang	Suburban agriculture	123.63	41.52	0.46±0.23	1.11±0.32